"Physics of Auroral Phenomena", Proc. XXXVIII Annual Seminar, Apatity, pp. 15-19, 2015

Polar Geophysical Institute

SUBSTORM INJECTION AT THEMIS SATELLITE AND NEAR-CONJUGATE AURORAL LUMINOSITY IN PRE-MIDNIGHT SECTOR: THE CASE STUDY

T.V. Kozelova, B.V. Kozelov *(Polar Geophysical Institute, Apatity, Russia)*

Abstract. We use spacecraft observations from THEMIS during a substorm on 19 Dec 2014, in conjunction with ground-based magnetic field observations and the aurora at the station Apatity , to examine the spatial structuring and temporal variability of the localized auroral intensification in pre-midnight sector. In this substorm the THEMIS at r ~ 7-9 R_E observed the high energetic particle injections and the sharp density decreases of less energetic particles simultaneously with the oscillations both with quasi-period of 30-40 s and the one oscillation with quasi-period of 2.5 min which occur near the substorm expansion phase onset. We discuss a possible association of particle dynamics and the magnetic and electric field variations during the substorm intensification.

1. Introduction

Lyons et al. [2003a] show that a reduction in equatorial plasma pressure within the current wedge simultaneous with the increase in energetic particle fluxes and dipolarization is a general feature of some substorms within the equatorial inner plasma sheet at 10–13 R_E. There have been very few direct measurements of the change in equatorial plasma pressure within the near-Earth plasma sheet during substorms [*Roux et al*., 1991; *Lui et al*., 1992]. Similar reduction in plasma pressure during the local dipolarization was observed by CRRES at ~6 R_E [*Kozelova et al*., 2003; *Kozelova et al*., 2006]. However, the contribution of this plasma pressure reduction in the current wedge formation (and thus in the substorm expansion phase) are not examined in detail.

Here we use spacecraft observations from THEMIS at 7-9 R_E during a substorm on 19 Dec 2014, in conjunction with the aurora observations at Apatity station (APT), to examine the spatial structure and temporal variability of the localized auroral intensification in pre-midnight sector.

2. Substorm evolutions

The evening of 19 December 2014 was characterized by long-lasting ground magnetic activity of 100–150 nT. Substorm auroral onset is identified by a brightening consisting of beading structure along the onset arc near APT at ~ 18:23 UT.

Fig. 2 shows from top to bottom: the auroral activity development (the auroral keograms) observed at APT, the magnetic field and the ion flux data observed at THD (panels *a*-*e*) and the *H* components at several ground-based stations during three activization 'A1'-'A3' (panels *f*-*h*). One can see westward propagation of the magnetic activity from DIK (the activization 'A1' on the panel *f*) to SOR (the activization 'A3' on the panel *h*). Thus, THD was located westward of the activization 'A1' site and eastward the activization 'A3'.

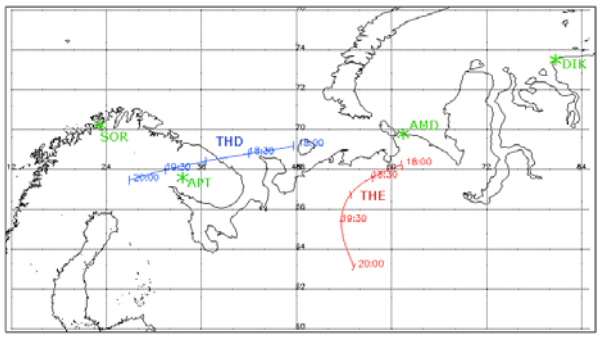

Figure 1. Location of the ground-based stations and the projections of the THD and THE satellites on 19 December 2014 at 18:00–20:00 UT.

From Fig. 2 one can see that each activization 'A1'-'A3' has such general features in the magnetosphere: the increase of the magnetic disturbances and the magnetic field dipolarization; a reduction in equatorial ion pressure simultaneously with the well-known expansion phase (EXP) increase in energetic particle fluxes (injections noted as *i*1-*i*3).

3. Initial substorm activization A1 dynamics

In this paper, we examine at detail the changes of the magnetic field and the ESA ion pressure within the equatorial inner plasma sheet at ~7–9 R_E during the first substorm activization A1. In this time besides THD, second satellite THE was located within sector between THD and substorm onset near the AMD meridian. In this interval the weak growth phase arc was oriented approximately in the east-west direction along the 68° latitude. The auroral beads propagate azimuthally westward and evolve into wavy structures, indicating that the beads are an auroral manifestation of onset waves. The arc brightenings were observed at the moments 't_1'=18:18 UT and 't_2'= 18:22 UT. Then at the moment T_{exp}=18:24 UT these wavy structures expand poleward more quick, indicating on the substorm expansion phase [*Voronkov et al.*, 2003].

E and B field oscillations in the magnetosphere. Fig. 3 presents the **E**- and **B**-field data at THD and THE. At this figure, the panels 'a'-'c' show the data at THD from top to bottom: the B_z component of the magnetic field and the E_x and E_y components of the electric field. The panels 'd'-'h' show the data at THE: the B_z component of the magnetic field; *Pi*2-like fluctuations of the magnetic field calculated as the deviations of observed

magnetic field from 108s-smoothed values, the most appreciable dB_x and dB_y components of the magnetic field is shown here; and also the E_x and E_y components of the electric field. Horizontal lines note the energetic ion injections observed at THD and THE. Vertical lines note the moments: 't_1','t_2' and T_{exp}.

From Fig. 3 one can see the oscillations of **B** and **E** field with several quasi-periods. Both before and after T_{exp}, the quasi-period of *1.5 min* (panels 'a' и 'f') has the signature at THD and THE. The oscillations with *quasi-period of 30-40 s* appear firstly at THE 1 min before T_{exp} and then – at THD on T_{exp}. Besides, the one oscillation with *quasi-period of 2.5 min* occurs at THE. For this oscillation at the interval 18:22-18:25 UT at THE (panels 'e' and 'h'), the perpendicular fluctuations of the magnetic field and the electric field *dBx* and *dEy* are ~90° out of phase as for *standing Alfvén waves* (SAW), which may be associated with intensification auroral arc near THE (r~6.8 R_E).

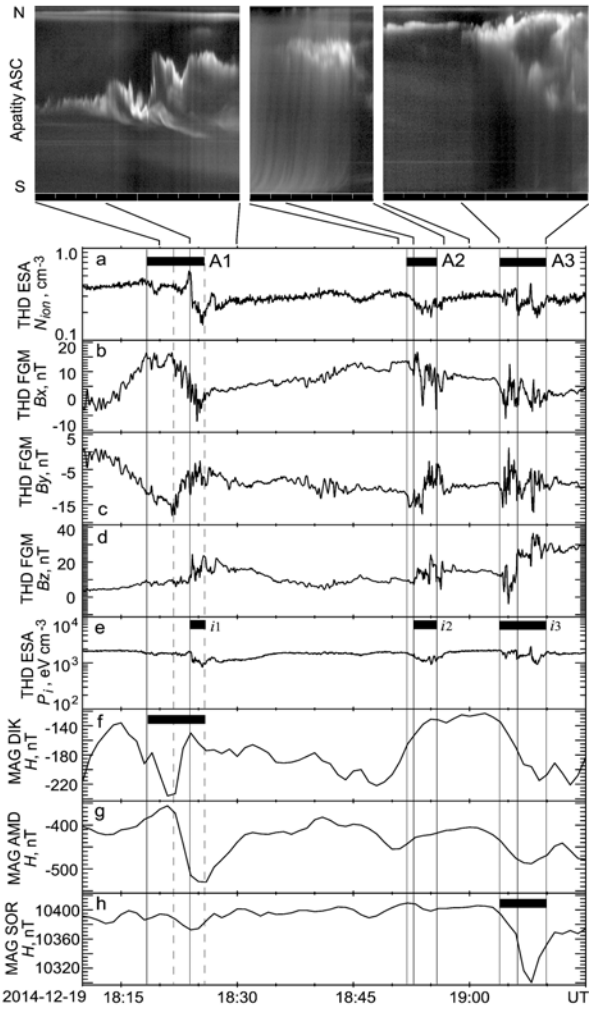

Figure 2. Ground-based and THD observations on 19 December 2014 at 18:00–20:00 UT.

Ion pressure gradient and upsurge in the duskward ion flux. Fig. 4 show from top to bottom the data at THD (panels 'a'-'f') and the data at THE (panels 'g'-'l'): the ion density (integrated from 5 eV to 25 keV); evolution of the electron spectrum (from 6 eV to 30 keV); three components of velocity of plasma flow (V_x, V_y, V_z) in GSM system and P_{xx} component of the ion pressure tensor.

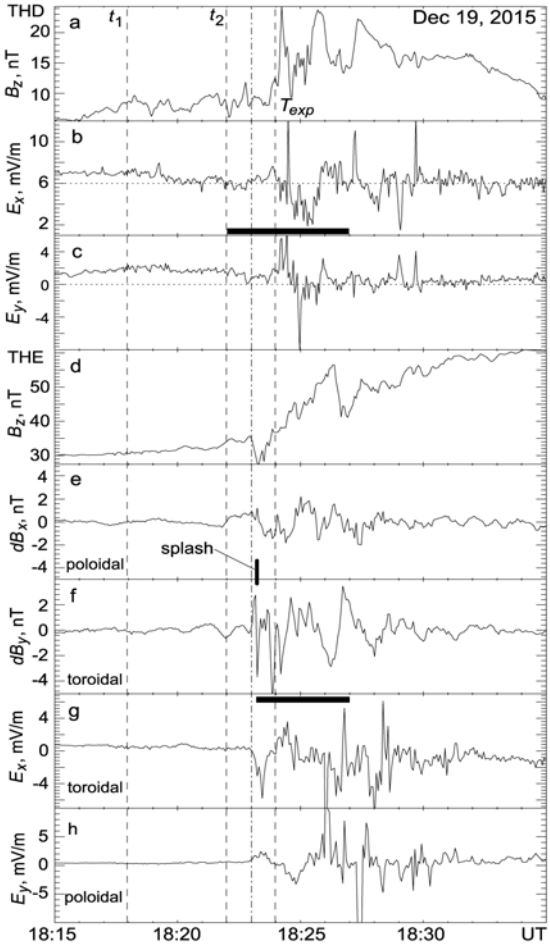

Figure 3. E- and **B**-field variation observed at THD and THE.

First, we consider the data at THD. After t_1, one can see weak increases in V_x and V_y, decrease of P_{xx} presure and weak the B_z increase. After T_{exp}, the sharp **drop** in the N_i and P_{xx} of ion are observed simultaneously with sharp **upsurge** in the duskward ion flux. These signatures coincide with the increase of electron E_{cut} from W_{cut} ~10 keV to W_{cut} ~ 20 keV (here W_{cut} is the cutoff energy), indicated that *new "fresh" electrons at the opened drift trajectories* convect toward the spacecraft position from the tail [*Kerns et al.*, 1994]. Simulteneously, the fluxes of "old" trapped electrons of 0.03–0.8 keV, which originated from previous activity, sharp decrease during the local dipolarization.

Now, we consider the data at THE (panels 'g'-'l'). Fig. 4 show slow increase in N_i and P_{xx} after t_1 and then (1 min before T_{exp}) sharp drop of the ion pressure and simulteneous sharp upsurge in the duskward ion drift velocity V_y. Pressure drop and the V_y upsurge last 30 s and were observed during rapid decrease of the magnetic field B_z component (magnetic field stretching) at THE. Sharp drop of the ion pressure during magnetic field stretching may indicate on the

increase of ion pressure gradient near the isotropic boundary for ions.

Short (10-15 s) **splash** of low-energy (0.1-1 keV) electrons occurs during the V_y upsurge maximum. This electron splash was accompanied by short (localized) the magnetic field dB_y variation with the change of dB_y sign, which can be interpreted as the field-aligned current $j_{||}$ transition by THE. After this 0.1-1 keV electron splash, the dipolarization at THE begins simultaneously with the electron pressure enhancement and the increase of electron E_{cut} from W_{cut} ~8 keV to W_{cut} ~ 28 keV.

Thus, we see similar structure of the phenomena observed by THE and THD, namely: sharp drop of the ion pressure and simulteneous sharp upsurge in the duskward ion drift velocity V_y. First, this structure was observed at THE at MLT=22.5, then - at more western THD at MLT=21.65. Judging from 60 s delay between THE and THD, this structure westward espanded with the velocity of 0.85 deg/min. This westward motion is slower than the azimuthal spreading of the onset arc brightening which occurs above APT ~ 30-40 s after t_1 at AMD. Besides, expansion-phase auroras also expand poleward and can contact an arc along the auroral poleward boundary, forming a bulge region that expands westward as the westward traveling surge. This westward motion is slower than the azimuthal spreading of the onset arc brightening as in [*Lyons et al.*, 2013].

4. Discussions

In this work the following important features of the particle and field variations in the magnetosphere during sharp **drop** of the ion pressure should be noted: sharp **upsurge** of the azimuthal flow (V_y) and **splash** of low-energy (0.1-1 keV) electrons. This phenomena associated with the **drop** of the ion pressure have not been observed before.

*We suppose that the sharp **upsurge** of the azimuthal flow (V_y) during sharp **drop** of the ion pressure may not be attributed to the **E** × **B** drift only but to pressure gradient also. If the azimuthal flow is mainly associated with the pressure gradient, the westward flow enhancements can be interpreted as pressure gradient enhancements in the z direction (earthward when mapped along field lines to the equatorial plane) that could lead to enhanced field-aligned currents and thus to the growth phase arc intensifications.

*Besides, short **splash** of low-energy electrons during the V_y upsurge maximum was accompanied by localized dB_y variation with the change of dB_y sign, which can be interpreted as the field-aligned current $j_{||}$ near THE.

The whole complex of above-mentioned phenomena supports the suggestion of Lyons et al., 2003b based on *particle divergence driven by magnetic drift,* for an explanation of the plasma pressure reduction during the current wedge formation.

Current wedge formation is expected to initiate in the region where the contours of constant P and V are not parallel, as illustrated in the left-hand panel of Fig. 5 (This is Fig. 3 from [*Lyons et al*., 2003b]), Here $V = \int ds/B$ is the flux tube volume per unit magnetic flux evaluated along field lines from the equator to the ionosphere. During longitudinally localized reduction in P, the cross-tail current reduction occurs in the plasma sheet, giving dipolarization of the magnetic field, which is accompanied by an increase in B_z and decrease in V. The decrease in P and in V will distort the contours of constant P and V as illustrated in the middle and right-hand panels of Fig. 5. This distortion of the contours is qualitatively as expected during current wedge forms. The particle divergence corresponds to a divergence in cross-tail current, which is related to field-aligned currents [*Birmingham*, 1992; *Lyons et al*., 2003b].

The component of the drift velocity V_d in the direction of ∇V gives particle divergence, and thus will give upward field-aligned currents. At Fig. 5 the asterisks note the expected sites of the satellites THE and THD. More favorable conditions for current $j_{||}$ observation were for THE.

5. Conclusions

We report a detailed case study of plasma pressure reduction during in the substorm expansion phase of substorm on December 19, 2014 using data from two THEMIS satellites in the evening sector magnetosphere. The following peculiarities of this event have been demonstrated:

- Pre-onset auroral waves, auroral beading and the magnetic field oscillations with the quasi-period of *1.5-2.5 min* and with *quasi-period of of 30-40 s,* observed at plasma sheet at 7-9 R_E, suggest that current disruption during the substorm is caused by plasma instabilities such as the ballooning instability and the cross-field current instability [Roux et al., 1991].
- **E**- and **B**-field variations, observed 1 min before T_{exp}, indicate on the appearance of SAW which may be associated with intensification auroral arc near THE (r~6.8 R_E).
- After T_{exp}, the sharp lasted 30 s **drop** in the N_i and P_{xx} of ion is observed simultaneously with sharp **upsurge** in the duskward ion velocity V_y.
- Short (10-15 s) **splash** of low-energy (0.1-1 keV) electrons occurs during the V_y upsurge maximum was accompanied by localized dBy variation with the change of dB_y sign, which can be interpreted as the field-aligned current $j_{||}$ near THE. The whole complex of above-mentioned phenomena has not been reported before.

Our results support and supplement the suggestion of *Lyons et al*., 2003b based on *particle divergence driven by magnetic drift,* for an explanation of the plasma pressure reduction during the current wedge formation. Pressure gradient enhancements may also provide a free-energy source for exciting the drift ballooning mode instability, which may also cause cross-tail current diversion.

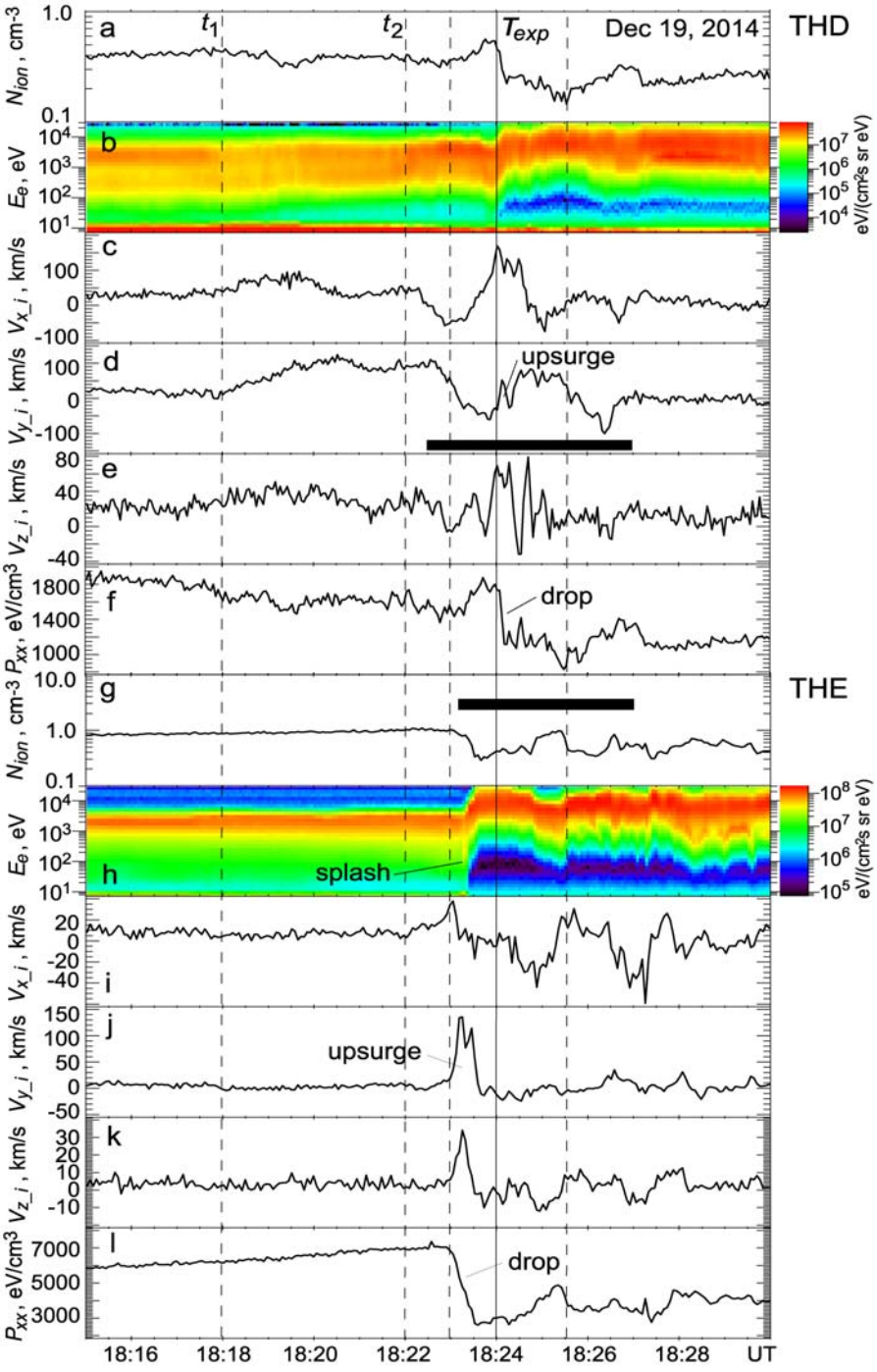

Figure 4. Dynamics of particles observed at THD and THE

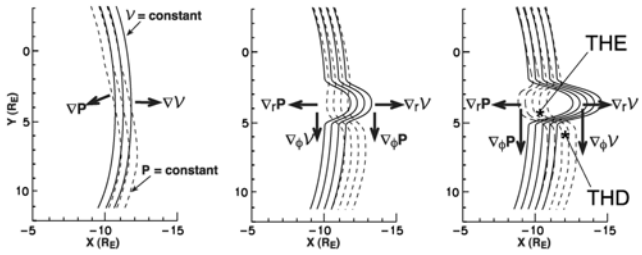

Figure 5. Schematic of current wedge formation, adopted from [*Lyons et al*., 2003b].

References

Birmingham, T.J. (1992), Birkeland currents in an anisotropic, magnetostatic plasma, *J. Geophys. Res*., 97, 3907.

Kerns, K.J., D.A. Hardy, and M.S. Gussenhoven (1994), Modeling of convection boundaries seen by CRRES in 120-eV to 28-keV particles, *J. Geophys. Res*., 99, 2403–2414.

Kozelova, T.V., L.L. Lazutin, B.V. Kozelov (2003), Particle diamagnetism and local dipolarization. *Geomagn. Aeronomy*, 43, 513-522.

Kozelova, T.V., B.V. Kozelov, L.L. Lazutin, (2006), Substorm low-energy particle decrease near the inner edge of the plasma sheet, 'Physics of Auroral Phenomena', *Proc. XXIX Annual Seminar*, Apatity, p. 96-99.

Lui, A.T. Y., R.E. Lopez, B.J. Anderson, K. Takahashi, L.J. Zanetti, R.W. McEntire, T.A. Potemra, D.M. Klumpar, E.M. Greene, and R. Strangeway (1992), Current disruptions in the near-Earth neutral sheet region, *J. Geophys. Res*., 97, 1461–1480, doi:10.1029/91JA02401

Lyons, L.R., C.-P. Wang, T. Nagai, T. Mukai, Y. Saito, and J.C. Samson, (2003a), Substorm inner plasma sheet particle reduction, *J. Geophys. Res*., 108(A12), 1426, doi:10.1029/2003JA010177.

Lyons, L.R., C.-P. Wang, and T. Nagai (2003b), Substorm onset by plasma sheet divergence, *J. Geophys. Res.*, 108(A12), 1427, doi:10.1029/2003JA010178.

Lyons, L.R., Y. Nishimura, B. Gallardo-Lacourt, Y. Zou, E. Donovan, S. Mende, V. Angelopoulos, J.M. Ruohoniemi, and K. McWilliams (2013), Westward traveling surges: Sliding along boundary arcs and distinction from onset arc brightening, *J. Geophys. Res. Space Physics*, 118, 7643–7653, doi:10.1002/2013JA019334.

Nishimura, Y., L.R. Lyons, S. Zou, X. Xing, V. Angelopoulos, S.B. Mende, J.W. Bonnell, D. Larson, U. Auster, T. Hori, N. Nishitani, K. Hosokawa, G. Sofko, M. Nicolls, and C. Heinselman. (2010), Preonset time sequence of auroral substorms: Coordinated observations by all-sky imagers, satellites, and radars, *J. Geophys. Res*., 115, A00I08, doi:10.1029/2010JA015832.

Roux, A., S. Perraut, P. Robert, A. Morane, A. Pedersen, A. Korth, G. Kremser, B. Aparicio, D. Rodger, and R. Pellinen (1991), Plasma sheet instability related to the westward traveling surge, *J. Geophys. Res.,* 96, 17,697–17,714, doi:10.1029/91JA01106.

Voronkov, I., E.F. Donovan, and J.C. Samson (2003), Observations of the phases of the substorm, *J. Geophys. Res.,* 108(A2), 1073, doi:10.1029/2002JA009314.